Synthesis of Tellurium Sorption Complexes in Fully Dehydrated and Fully Ca^{2+}-exchanged Zeolites A and X and their Single-crystal Structures

Woo Taik Lim,* Jong Sam Park,† Sang Hoon Lee,‡ Ki Jin Jung,‡ and Nam Ho Heo‡,*

*Department of Applied Chemistry, Andong National University, Andong 760-749, Korea. *E-mail: wtlim@andong.ac.kr*
†Department of Radiologic Technology, Daegu Health College, Daegu 702-722, Korea
*‡Department of Applied Chemistry, Kyungpook National University, Daegu 702-701, Korea. *E-mail: nhheo@knu.ac.kr*
Received March 31, 2009, Accepted April 17, 2009

Single crystals of fully dehydrated and fully Ca^{2+}-exchanged zeolites A ($|Ca_6|[Si_{12}Al_{12}O_{48}]$-LTA) and X ($|Ca_{46}|[Si_{100}Al_{92}O_{384}]$-FAU) were brought into contact with Te in fine pyrex capillaries at 623 K and 673 K, respectively, for 5 days. Crystal structures of Te-sorbed Ca^{2+}-exchanged zeolites A and X have been determined by single-crystal X-ray diffraction techniques at 294 K in the cubic space group $Pm\bar{3}m$ (a = 12.288(2) Å) and $Fd\bar{3}$ (a = 25.012(1) Å), respectively. The crystal structures of pale red-brown $|Ca_6Te_3|[Si_{12}Al_{12}O_{48}]$-LTA and black coloured $|Ca_{46}Te_8|[Si_{100}Al_{92}O_{384}]$-FAU have been refined to the final error indices of R_1/wR_2 = 0.1096/0.2768 and R_1/wR_2 = 0.1054/0.2979 with 204 and 282 reflections for which $F_o > 4\sigma(F_o)$, respectively. In the structure of $|Ca_6Te_3|[Si_{12}Al_{12}O_{48}]$-LTA, 6 Ca^{2+} ions per unit cell were found at one crystallographic positions, on 3-fold axes equipoints of opposite 6-rings. In $|Ca_{46}Te_8|[Si_{100}Al_{92}O_{384}]$-FAU, 46 Ca^{2+} ions per unit cell were found at four crystallographically distinct positions: 3 Ca^{2+} ions at Ca(1) fill the 16 equivalent positions of site I, 21 Ca^{2+} ions at Ca(2) fill the 32 equivalent positions of site I', 10 and 12 Ca^{2+} ions at Ca(3) and Ca(4), respectively, fill the 32 equivalent positions of site II. The Te clusters are stabilized by interaction with cations and framework oxygen. In sodalite units, Te-Te distances of 2.86(10) and 2.69(4) Å in zeolites A and X, respectively exhibited strong covalent properties due to their interaction with Ca^{2+} ions. On the other hand, in large cavity and supercage, those of 2.99(3) and 2.76(11) Å in zeolites A and X, respectively, showed ionic properties because alternative ionic interaction was formed through framework oxygen at one end and Ca^{2+} cations at the other end.

Key Words: Zeolite A, Zeolite X, Tellurium, Ca^{2+}, Structure

Introduction

Semiconductor nanoparticles have been the subject of intensive investigation over the past several years.[1-4] Semiconductor nanoparticles have aroused renewed interest because of their interesting physics and the potential of unique applications as photocatalysts for solar energy conversion, media for optical information or image storage, electronics, nonlinear optics, electroluminescent displays, and photoluminescent sensors, and so on.[5-7] The progression of electronic and optical properties of these semiconductor particles from bulk-like to molecular, as their size is decreased, is now well understood theoretically.[8-12]

The physical and chemical properties of semiconductors change markedly in the nanometer size regime, because the ratio of surface-to-bulk atoms increases with decreasing size.[1,8,10] The high surface free energy of these nanoclusters is manifested in unusual crystal structure transformation and particle shapes, as well as enhanced reactivity.[1,9] Control of the surface chemistry is a necessary prerequisite to nanoparticle synthesis and is also important in all of the potential applications mentioned above.

Especially, porous structures such as zeolites, which are three dimensional, about 30% ~ 50% void space after dehydration, crystalline solids with well defined structures that contain aluminum, silicon, and oxygen in their regular framework, provide a mechanism for confining materials in a controlled fashion, lending themselves to a wide range of applications.[4] A number of recent papers deal with the introduction of chalcogen elements like as S, Se, and Te into channels of different zeolites.[3,9-11,13-18] These chalcogen elements are widely used as electronics (xerographic plates, TV cameras, photocells, magnetic computer cores, solar batteries, rectifiers, and relays), ceramics (colorant for glass), steel and copper (degasfier and machinability improver), rubber accerlerator, catayst, and trace element in animal feeds.[19]

V. N. Bogomolov *et al.*[13] investigated the absorption spectra of a regular system of 12 Å particles-clusters of Se in the zeolites A and X. They claimed that depending on the type of zeolites, Na-A or Na-X, the system of clusters formed a diamond-type lattice, or a primitive cubic lattice, respectively. It was suggested in that an interaction exists between the cluster, *i.e.*, that secondary crystals were produced with corresponding collective properties. They also reported that unfortunately, they still did not know the detailed structure of the clusters and if an individual cluster in a zeolite cavity was regarded as microcrystal, then the latter was probably under the conditions of the quantum size effect.

V. N. Bogomolov *et al.*[14] also synthesized the known stable and unstable phases of S, Se, and Te elements by way of production of clusters in cavities of zeolites in Na-A and Na-X. They identified an unknown tellurium modification, a Te_8 ring, by the spectra of Raman scattering of light.

A. I. Zadorozhnii *et al.*[8] extensively studied the dependence of the magnetic properties of selenium and tellurium on the degree of dispersion. They obtained particles with the number

of atoms ranging from 2 to 20 in the voids of zeolites A and X, by adsorption method. Their experiments showed that for small fillings (from 1 to 7 Se atoms/void in Na-A, and from 1 to 4 Se atoms/void in Na-X) a paramagnetic signal was observed which changes into a diamagnetic signal for large fillings.

On the basis of Raman spectra, Vladimir V. Poborchii[20] discussed the structures of sulfur, selenium, and tellurium clusters confined in the large cavities of zeolite A. He proposed that sulfur, selenium, and tellurium clusters were stabilized in the forms of S_8, Se_8 (or Se_{12}), Te_8 rings, respectively.

The measurements of the extended X-ray absorption fine structure and the photoacoustic spectroscopy was carried out for Se chains confined in the channels of synthetic modenite with about 6.7 Å diameter by Kozaburo Tamura *et al.*[11] They reported the first-nearest Se-Se distances in mordenite channels was 2.32 Å, shorter than that in crystalline Se, and then proposed the isolated Se chains in the mordenite channels were strongly photo-sensitive.

John B. Parise *et al.*[3] characterized the Se-loaded zeolites A, X, Y, AlPO-5, and Mordenite by using EXAFS, solid-state NMR, and diffuse-reflectance techniques. Their studies revealed selenium was predominantly of the helical chain form, a mixture of allotropes and helical chain form, and a fixed-pitch helical-chain allotrope in the Na-A, Na-X, Na-Y, mordenite, and AlPO-5.

Y. Nozue *et al.*[21] studied the Se adsorbed in faujasite (X or Y) as a function of x, where x was the Al-to-(Al + Si) ratio by absorption spectra. They reported that the amount of adsorbed Se increased with increasing x for small x and was saturated for $x \geq 0.1$. These results were interpreted using the model in which the finite number of Se atoms was physically adsorbed by each permanent dipole which consists of $(AlO_4)^-$ in a zeolite framework and cation.

In order to study how the different Se composition in the samples affect the properties of prepared Se_8-ring clusters, Z. Lin *et al.*[22] investigated the loaded Se in zeolite 5A by use of the absorption and Raman spectra. They reported that single Se_8-ring clusters and double Se_8-ring clusters could be formed in the cages of zeolite 5A and in Se_8-ring clusters, there was strong coupling between electrons and phonons, and the optical absorption was the absorption of the strong electron-phonon coupling quantum system.

As mentioned above, most of the work focused on the selenium clusters in various zeolites by using absorption and Raman spectroscopy,[9-11,13-22] so the structural information on tellurium clusters in the cavities of zeolite were less clear. In this work, fully Ca^{2+}-exchanged zeolites A ($|Ca_6|[Si_{12}Al_{12}O_{48}]$-LTA) and X ($|Ca_{46}|[Si_{100}Al_{92}O_{384}]$-FAU) were treated with tellurium in an attempt to synthesize nanoclusters of tellurium within the zeolites A and X. The crystal structures of the resulting products were determined to verify that nanoclusters had formed, to learn their positions, size, and geometry, and to observe their interactions with the zeolite framework.

Experimental Section

Preparation of Fully Ca^{2+}-exchanged Zeolites A and X. Large colorless single crystals of hydrated $|Na_{12}|[Si_{12}Al_{12}O_{48}]$-LTA (or Na_{12}-A) and $|Na_{92}|[Si_{100}Al_{92}O_{384}]$-FAU (or Na_{92}-X) were synthesized by Charnell[23] and Petranovskii,[24] respectively. Colourless single crystals of zeolites A and X, about 0.06 mm and 0.15 mm in cross-section, respectively, were lodged in a fine Pyrex capillary. Crystals of hydrated $|Ca_6|[Si_{12}Al_{12}O_{48}]$-LTA and $|Ca_{46}|[Si_{100}Al_{92}O_{384}]$-FAU were prepared by the dynamic (flow) ion-exchange of Na-A and Na-X with an exchange solution of 0.04325 M $Ca(NO_3)_2$ (Aldrich 99.997%) and 0.00675 M CaO (Aldrich 99.995%) with a total concentration of 0.05 M. CaO was added to the exchange solution to increase its pH because the frameworks of zeoslite crystals are usually destroyed by hydronium ions. The crystals of colorless $|Ca_6|[Si_{12}Al_{12}O_{48}]$-LTA and $|Ca_{46}|[Si_{100}Al_{92}O_{384}]$-FAU were completely dehydrated at 623 K, 673 K and 2×10^{-6} Torr for 48 hr., respectively.

Synthesis of Tellurium Sorption Complex in Zeolites A and X. The crystals of fully dehydrated $|Ca_6|[Si_{12}Al_{12}O_{48}]$-LTA and $|Ca_{46}|[Si_{100}Al_{92}O_{384}]$-FAU were brought into contact with Te (Aldrich 99.999%) under vacuum in fine Pyrex capillaries at 573 K and 673 K, respectively, for 5 days. These were

Tale 1. Summary of Experimental and Crystallographic Data

	$\|Ca_6Te_3\|[Si_{12}Al_{12}O_{48}]$-LTA (crystal 1)	$\|Ca_{46}Te_8\|[Si_{100}Al_{92}O_{384}]$-FAU (crystal 2)
Crystal cross-section (mm)	0.06	0.15
Ion exchange for Ca^{2+} (days, °C)	3, 8.0	5, 12.0
Dehydration (days, °C)	2, 350	3, 400
Reaction with Te (days, °C)	5, 350	5, 400
Temperature for data collection (°C)	21	21
Radiation (Mo $K\alpha$) λ_1	0.70930	0.70930
λ_2	0.71359	0.71359
Space group	$Pm\bar{3}m$	$Fd\bar{3}$
Unit cell constant, a (Å)	12.288(2)	25.012(1)
2θ range for a (deg)	20-30	10-20
Scan technique	ω - 2θ	ω - 2θ
Scan width (deg)	0.78+1.50*tan(θ)	0.47+0.62*tan(θ)
No. of reflection for a	15	25
2θ range in data collection	2-70	2-50
No. of reflections measured	877	1239
No. of unique reflections, m	877	1045
No. of reflections ($F_o > 4\sigma(F_o)$)	204	282
No. of parameters, s	33	73
Data / parameter ratio	26.6	14.3
Weighting parameters : a/b	0.0566/100.3451	0.1289/400.2351
R_1[a] ($F_o > 4\sigma(F_o)$)	0.1096	0.1054
wR_2[b] (intensities)	0.2768	0.2979
Goodness of fit[c]	1.018	1.211

[a] $R_1 = \Sigma||F_o|-|F_c||/\Sigma|F_o|$ [b] $wR_2 = [\Sigma w(F_o^2-F_c^2)^2/\Sigma w(F_o^2)^2]^{1/2}$; R_1 and wR_2 are calculated using only the 204 and 282 reflections for which $F_o > 4\sigma(F_o)$, for crystal 1 and 2, respectively. [c] Goodness of fit = $(\Sigma w(F_o^2-F_c^2)^2/(m-s))^{1/2}$, where m and s are the number of unique reflections and variables, respectively.

achieved by condensing Te on and near the crystals from a Te source at 623 K and 723 K for $|Ca_6|[Si_{12}Al_{12}O_{48}]$-LTA and $|Ca_{46}|[Si_{100}Al_{92}O_{384}]$-FAU, respectively, in a coaxially connected heating oven.

The temperature of the Te source was then lowered to below 523 K; after 24 h the Te droplets near the zeolite crystals were no longer seen. The resulting crystals, still under vacuum in their capillaries, were pale red-black and black for crystals 1 and 2, respectively.

X-ray Data Collection. The cubic space group $Pm\bar{3}m$ (no systematic absences) for zeolite A (crystal 1) was used in this work for reasons discussed previously.[25,26] In the case of zeolite X (crystal 2), the cubic space group $Fd\bar{3}$ was used throughout this work; intensity inequalities for *hkl* and *khl* support this choice. This space group had been found to be correct for many other crystals from the same batch.[27]

A CAD4/Turbo diffractometer equipped with a rotating anode generator and a graphite monochromator was used for preliminary experiments and for the subsequent collection of diffraction intensities, all at 294 K and 1 atm using molybdenum radiation. For each crystal, the cell constants, a = 12.288(2) Å and 25.012(1) Å, respectively for crystals 1 and 2, were determined by a least-squares treatment of 15 and 25 intense reflections for crystals 1 and 2, respectively, in diverse regions of reciprocal space. Each reflection was scanned at a constant scan speed of 0.5°/min in 2θ with a scan width of $(0.78 + 1.50 \tan\theta)$ and $(0.47 + 0.62 \tan\theta)$, for crystals 1 and 2, respectively. Background intensity was counted at each end of a scan range for a time equal to half the scan time. The intensities of three reflections in diverse regions were recorded every 3 hours to monitor crystal and instrumental stability. Only small random fluctuations of these check reflections were observed during the course of data collection. Absorption corrections (μR *ca*. 0.24 and 2.20 for crystals 1 and 2, respectively) were made using the semiempirical Ψ-scan method. The corrected data gave nearly the same final R values, so the corrections were not used. Other experimental details as well as a summary of the crystallographic data are given in Table 1.

Structure Determination

$|Ca_6Te_3|[Si_{12}Al_{12}O_{48}]$-LTA (Crystal 1). Full-matrix least-squares refinement (SHELXL97)[28] was initiated with the atomic parameters of the framework atoms [(Si,Al), O(1), O(2), and O(3)] in dehydrated $|Na_{12}|[Si_{12}Al_{12}O_{48}]$-LTA.[29] The initial refinement using isotropic thermal parameters for all positions converged to the error indices $R_1 = 0.2916$ and $wR_2 = 0.6945$. (See Table 2, footnotes.) Refinement including the Ca(1)

Table 2. Positional, Thermal, and Occupancy Parameters[a] of $|Ca_6Te_3|[Si_{12}Al_{12}O_{48}]$-LTA and $|Ca_{46}Te_8|[Si_{100}Al_{92}O_{384}]$-FAU

	Wyckoff position	x	y	z	U_{11} or U_{iso}[b]	U_{22}	U_{33}	U_{23}	U_{13}	U_{12}	Occupancy[c] fixed	Occupancy[c] varied
$|Ca_6Te_3|[Si_{12}Al_{12}O_{48}]$-LTA, crystal 1												
(Si,Al)	24(*k*)	0	1843(3)	3733(3)	12(2)	13(2)	9(2)	1(1)	0	0	24[d]	
O(1)	12(*h*)	0	2337(7)	5000[e]	33(8)	18(7)	11(6)	0	0	0	12	
O(2)	12(i)	0	2829(7)	2829(7)	58(10)	12(4)	12(4)	11(6)	0	0	12	
O(3)	24(*m*)	1121(5)	1121(5)	3471(7)	19(3)	19(3)	36(6)	-2(3)	-2(3)	8(4)	24	
Ca(1)	8(*g*)	1946(5)	1946(5)	1946(5)	66(4)	66(4)	66(4)	42(4)	42(4)	42(4)	6	5.77(13)
Te(1)	8(*g*)	3089(13)	3089(13)	3089(13)	108(9)						1	1.17(10)
Te(2)	8(*g*)	807(19)	807(19)	807(19)	263(28)						1	1.01(10)
Te(3)	24(*l*)	1764(38)	3812(38)	5000[e]	125(16)						1	1.04(13)
$|Ca_{46}Te_8|[Si_{100}Al_{92}O_{384}]$-FAU, crystal 2												
Si	96(*g*)	-529(2)	1247(3)	358(2)	9(3)	17(3)	7(3)	-8(3)	4(2)	-7(3)	96	
Al	96(*g*)	-545(2)	368(2)	1240(3)	19(3)	25(3)	29(3)	-7(4)	-7(3)	5(3)	96	
O(1)	96(*g*)	-1068(6)	-13(6)	1026(6)	4(11)	32(9)	49(11)	-4(9)	2(9)	-10(8)	96	
O(2)	96(*g*)	-17(6)	-21(6)	1430(6)	34(10)	32(10)	42(11)	-6(8)	0(8)	6(8)	96	
O(3)	96(*g*)	-316(6)	741(6)	708(6)	44(10)	23(9)	35(10)	13(8)	24(9)	8(8)	96	
O(4)	96(*g*)	-691(5)	748(6)	1777(5)	21(8)	38(9)	21(9)	-25(7)	-2(7)	3(8)	96	
Ca(1)	16(*c*)	0[f]	0	0	25(15)						3	2.7(6)
Ca(2)	32(*e*)	684(3)	684(3)	684(3)	26(3)						21	22.2(11)
Ca(3)	32(*e*)	2204(8)	2204(8)	2204(8)	45(9)						10	9.9(11)
Ca(4)	32(*e*)	2481(10)	2481(10)	2481(10)	85(10)						12	9.1(13)
Te(1)	32(*e*)	1632(8)	1632(8)	1632(8)	85(11)						4	3.8(2)
Te(2)	96(*g*)	3448(47)	3401(49)	2019(50)	90(43)						2	2.6(4)
Te(3)	96(*g*)	2691(37)	2591(32)	2895(30)	34(22)						2	2.4(4)

[a]Positional parameters × 10^4 and anisotropic thermal parameters × 10^3 are given. Numbers in parentheses are the estimated standard deviations in the units of the least significant figure given for the corresponding paremeter. The anisotropic temperature factor is $\exp[-2\pi^2 a^{-2}(U_{11}h^2 + U_{22}k^2 + U_{33}l^2 + 2U_{12}hk + 2U_{13}hl + 2U_{23}kl)]$. [b]Isotropic thermal parameter in units of Å^2. [c]Occupancy factors are given as the number of atoms or ions per unit cell. [d]Occupancy for (Si) = 12 and (Al) = 12. [e]Exactly 0.5 by symmetry. [f]Fixed by symmetry.

Table 3. Selected Interatomic Distances (Å) and Angles (deg)[a] in $|Ca_6Te_3|[Si_{12}Al_{12}O_{48}]$-LTA and $|Ca_{46}Te_8|[Si_{100}Al_{92}O_{384}]$-FAU

Distances		Angles	
	$|Ca_6Te_3|[Si_{12}Al_{12}O_{48}]$-LTA, crystal 1		
(Si,Al)-O(1)	1.67(11)	O(1)-(Si,Al)-O(2)	111.2(6)
(Si,Al)-O(2)	1.64(2)	O(1)-(Si,Al)-O(3)	112.0(4)
(Si,Al)-O(3)	1.67(2)	O(2)-(Si,Al)-O(3)	105.1(4)
		O(3)-(Si,Al)-O(3)	111.1(6)
Ca(1)-O(3)	2.360(11)		
Ca(1)-Te(1)	2.43 (3)	O(3)-Ca(1)-O(3)	119.90(10)
Ca(1)-Te(2)	2.42 (4)		
		Ca(1)-Te(2)-Te(2)	125.30(10)
Te(2)-Te(2)	2.86(10)	Ca(1)-Te(1)-Te(3)	108.1(10)
Te(1)-Te(3)	2.99(3)	Te(1)-Te(3)-Te(1)	103.4(16)
Te(3)-O(1)	2.82(5)	Te(1)-Te(3)-O(1)	103.1(11)
		Te(2)-Te(2)-Te(2)	60[b]
	$|Ca_{46}Te_8|[Si_{100}Al_{92}O_{384}]$-FAU, crystal 2		
Si-O(1)	1.581(15)	O(1)-Si-O(2)	111.8(8)
Si-O(2)	1.647(15)	O(1)-Si-O(3)	109.7(9)
Si-O(3)	1.631(15)	O(1)-Si-O(4)	109.2(8)
Si-O(4)	1.614(13)	O(2)-Si-O(3)	105.9(8)
mean Si-O	**1.618(15)**	O(2)-Si-O(4)	107.3(8)
		O(3)-Si-O(4)	112.9(8)
Al-O(1)	1.705(14)	O(1)-Al-O(2)	111.2(8)
Al-O(2)	1.707(15)	O(1)-Al-O(3)	108.5(8)
Al-O(3)	1.720(14)	O(1)-Al-O(4)	113.3(8)
Al-O(4)	1.685(13)	O(2)-Al-O(3)	105.4(8)
mean Al-O	**1.704(14)**	O(2)-Al-O(4)	105.6(8)
		O(3)-Al-O(4)	112.7(8)
Ca(1)-O(3)	2.677(16)	Si-O(1)-Al	139.9(10)
Ca(2)-O(3)	2.500(17)	Si-O(2)-Al	143.4(10)
Ca(2)-Te(1)	2.458(14)	Si-O(3)-Al	136.3(11)
Ca(3)-Te(1)	2.479(4)	Si-O(4)-Al	147.0(10)
Ca(3)-O(2)	2.233(15)		
Ca(3)-Te(3)	2.26(7)	O(3)-Ca(1)-O(3)	93.4(5)
Ca(4)-O(2)	2.62(3)	O(3)-Ca(2)-O(3)	94.5(7)
		O(2)-Ca(3)-O(2)	119.2(3)
Te(1)-Te(1)	2.69(4)	O(2)-Ca(4)-O(2)	94.8(13)
Te(2)-Te(3)	2.760(11)		
Te(2)-O(1)	3.27 (7)	Ca(2)-Te(1)-Te(1)	105.5(6)
		Te(1)-Te(1)-Ca(3)	144.70(10)
		Te(1)-Te(1)-Te(1)	60[b]
		Ca(3)-Te(3)-Te(2)	105.5(5)
		Te(3)-Te(2)-O(1)	114.2(22)

[a]The numbers in parentheses are the estimated standard deviations in the units of the least significant digit given for the corresponding parameters. [b]Exactly 60° by symmetry.

Table 4. Deviations (Å) of Atoms from Six-ring Planes in $|Ca_6Te_3|[Si_{12}Al_{12}O_{48}]$-LTA and $|Ca_{46}Te_8|[Si_{100}Al_{92}O_{384}]$-FAU

Ions or Atoms	Charge	Distance
	$|Ca_6Te_3|[Si_{12}Al_{12}O_{48}]$-LTA, crystal 1	
	at O(3)[a]	
Ca(1)	+2	-0.10
Te(1)	0	-2.53
Te(2)	0	2.32
	$|Ca_{46}Te_8|[Si_{100}Al_{92}O_{384}]$-FAU, crystal 2	
	at O(3)[b]	
Ca(2)	+2	1.34
Te(1)	0	-2.27
	at O(2)[c]	
Ca(3)	+2	0.20
Ca(4)	+2	1.33

[a]A positive deviation indicates that the ion lies on the same side of the plane as the origin, *i.e.*, inside the sodalite unit of zeolite A. [b]A positive deviation indicates that ion lies in the sodalite unit of zeolite X. [c]A positive deviation indicate that ion or atom lies in the supercage of zeolite X.

position at a peak (0.1885, 0.1885, 0.1885, opposite a 6-ring in the sodalite unit) from the initial difference Fourier function led to convergence with $R_1 = 0.1762$ and $wR_2 = 0.5183$ and an occupancy of 5.97(21) Ca^{2+} ions. The next difference Fourier function (based on this model) revealed a peak at (0.3093, 0.3093, 0.3093), opposite a 6-ring in the large cavity. Refinement including this peak as Te(1) converged to $R_1 = 0.1515$ and $wR_2 = 0.4908$, with occupancies of 5.67(21) and 1.01(10) for Ca(1) and Te(1), respectively. The addition of another peak at Te(2) (0.0842, 0.0842, 0.0842, inside the sodalite unit) reduced the error indices to $R_1 = 0.1413$ and $wR_2 = 0.4598$, with occupancies of 5.59(19), 1.12(10), and 0.92(20) for Ca(1), Te(1), and Te(2), respectively. A subsequent refinement included Te(3), a peak found opposite a 4-ring in the large cavity at (0.1807, 0.3845, 0.5), led to $R_1 = 0.1322$ and $wR_2 = 0.3757$, with occupancies of 5.71(16), 1.31(10), 1.10(11), and 1.12(17) for isotropically refined Ca(1), Te(1), Te(2), and Te(3), respectively. A subsequent refinement with anisotropic thermal parameters for Ca^{2+} ion at Ca(1) converged to $R_1 = 0.1094$ and $wR_2 = 0.2880$ with occupancies of 5.77(13), 1.17(10), 1.01(10), and 1.04(13) for Ca(1), Te(1), Te(2), and Te(3). The final cycles of refinement with occupancies of 6.0, 1.0, 1.0, and 1.0 at Ca(1), Te(1), Te(2), and Te(3), respectively, as shown in Table 2 converged to $R_1 = 0.1096$ and $wR_2 = 0.2768$ with anisotropic thermal parameters for all framework and cations except for Te(1), Te(2), and Te(3). The final difference Fourier function was featureless; the notation $|Ca_6Te_3|[Si_{12}Al_{12}O_{48}]$-LTA will be used for this crystal. All shifts in the final cycles of refinement were less than 0.1% for the corresponding estimated standard deviations. The final structural parameters are given in Table 2. Selected interatomic distances and angles are given in Table 3.

Fixed weights were used initially; the final weights were assigned using the formula $w = 1/[\sigma^2(F_o^2) + (aP)^2 + bP]$ where $P = [\mathrm{Max}(F_o^2,0) + 2F_c^2]/3$, with $a = 0.056$ and $b = 100.3451$ as refined parameters (see Table 1). Atomic scattering factors for Ca^{2+}, Te, and $(Si,Al)^{1.75+}$ were used.[30,31] The function describing $(Si,Al)^{1.75+}$ is the mean of the Si^{4+}, Si^0, Al^{3+}, and Al^0 functions. All scattering factors were modified to account for anomalous dispersion.[32,33]

$|Ca_{46}Te_8|[Si_{100}Al_{92}O_{384}]$-FAU (Crystal 2). Full-matrix least-squares refinement (SHELXL97)[28] was initiated with the atomic parameters of the framework atoms [(Si,Al), O(1), O(2), O(3), and O(4)] in dehydrated $|Rb_{71}Na_{21}|[Si_{100}Al_{92}$

O_{384}]-FAU.[34] The initial refinement using isotropic thermal parameters for all positions converged to the error indices R_1 = 0.2684 and wR_2 = 0.5970. (See Table 2, footnotes.) Introducing Ca(1) as Ca^{2+} cations at a peak (0.0, 0.0, 0.0, site I) from a difference Fourier function reduced R_1 = 0.2586 and wR_2 = 0.5837 with resulting occupancy of 6.6(14) at Ca(1). The addition of another peak at Ca(2) (0.06, 0.06, 0.06, opposite a 6-ring in the hexagonal prism) from the difference Fourier function led to convergence with R_1 = 0.1782 and wR_2 = 0.4650 and an occupancies of 4.5(9) and 21.2(15) for Ca(1) and Ca(2), respectively. The next difference Fourier function (based on this model) revealed a peak at (0.22, 0.22, 0.22), opposite a 6-ring in the supercage (site II). Refinement including this peak as Ca(4) converged to R_1 = 0.1597 and wR_2 = 0.4015, with occupancies of 2.4(7), 22.1(12), and 20.2(20) for Ca(1), Ca(2), and Ca(4), respectively. Refinement including the Ca(3) position at a peak (0.21, 0.21, 0.21) from the another difference Fourier function led to convergence with R_1 = 0.1379 and wR_2 = 0.3743 and an occupancies of 2.7(6), 22.2 (11), 9.9(11), and 9.1(13) for Ca(1), Ca(2), Ca(3), and Ca(4), respectively. All Ca positions were refined isotropically in the cycles of refinement with occupancies fixed at 3, 21, 10, and 12 at Ca(1), Ca(2), Ca(3), and Ca(4), respectively. This converged to the error index R_1 = 0.1372 and wR_2 = 0.3758. A subsequent difference Fourier function based on this model revealed a peak in the sodalite unit at (0.1669, 0.1669, 0.1669). Refinement including this peak as Te(1) with anisotropic thermal parameters for all framework atoms converged to R_1 = 0.1208 and wR_2 = 0.3294 with occupancies of 3 (fixed), 21 (fixed), 10 (fixed), 12 (fixed), and 5.8(5) at Ca(1), Ca(2), Ca(3), Ca(4), and Te(1), respectively. Another difference Fourier function based on a model revealed a peak at (0.345, 0.340, 0.202) on a slightly off 3-fold axis opposite a 6-ring in the supercage. The following refinement including this peak as Te(2) converged with R_1 = 0.1165 and wR_2 = 0.3250 and occupancies of 3 (fixed), 21 (fixed), 10 (fixed), 12 (fixed), 3.7(2), and 2.1(4) at Ca(1), Ca(2), Ca(3), Ca(4), Te(1), and Te(2), respectively. A subsequent refinement including a peak found in the supercage at (0.26, 0.25, 0.28) as Te(3) further reduced the error indices to R_1 = 0.1125 and wR_2 = 0.3250, with a refined occupancies of 3 (fixed), 21 (fixed), 10 (fixed), 12 (fixed), 3.8(2), 2.6(4), and 2.4(4) at Ca(1), Ca(2), Ca(3), Ca(4), Te(1), Te(2), and Te(3), respectively. The final refinement with anisotropic thermal parameters for all atoms except for isotropic thermally refined with all occupancies fixed at 3, 21, 10, 12, 4, 2, and 2 at Ca(1), Ca(2), Ca(3), Ca(4), Te(1), Te(2), and Te(3), respectively, converged to R_1 = 0.1054 and wR_2 = 0.2979. The difference Fourier function based on this model was featureless except for some peaks in the supercage. Efforts to introduce those peaks as Te species were unsuccessful; they were always unstable in refinement. The notation $|Ca_{46}Te_8|[Si_{100}Al_{92}O_{384}]$-FAU will be used for this crystal. All shifts in the final cycles of refinement were less than 0.1% for the corresponding estimated standard deviations. The final structural parameters are presented in Table 2, and selected interatomic distances and angles are in Table 3.

Fixed weights were used initially; the final weights were assigned using the formula $w = 1/[\sigma^2(F_o^2) + (aP)^2 + bP]$ where $P = [\mathrm{Max}(F_o^2,0) + 2F_c^2]/3$, with a = 0.1289 and b = 400.2351 as refined parameters (see Table 1). Atomic scattering factors for Ca^{2+}, Te, and $(Si,Al)^{1.75+}$ were used.[30,31] The function describing $(Si,Al)^{1.75+}$ is the mean of the Si^{4+}, Si^0, Al^{3+}, and Al^0 functions. All scattering factors were modified to account for anomalous dispersion.[32,33]

Result and Discussion

Crystal Structure of $|Ca_6Te_3|[Si_{12}Al_{12}O_{48}]$-LTA (Crystal 1). In the crystal structure of Te-sorbed Ca^{2+}-exchanged zeolite A ($|Ca_6Te_3|[Si_{12}Al_{12}O_{48}]$-LTA), each unit cell contained six Ca^{2+} ions at Ca(1) all located at one crystallograhphically distinct position, all near the centers of 6-rings on the 3-fold axes. These Ca^{2+} ions extends about 0.10 Å into the large cavity from the (111) plane at O(3) and are coordinated to three O(3) oxygens at 2.360(11) Å (see Tables 3 and 4). Considering that the sum of ionic radii of Ca^{2+} and O^{2-} is 0.99 + 1.32 = 2.31 Å,[35] the Ca(1)-O(3) approach distances, 2.360(11) Å, are very reasonable. The O(3)-Ca(1)-O(3) angles are close to 120° (119.90(10)°), so the Ca^{2+} ions are nearly trigonal-plannar (see Table 3).

In this work, a total of three sorbed Te atoms per unit cell were found at two different 3-fold positions and at 24-fold positions. Two Te atoms per unit cell were found at Te(1) and Te(2) on the 3-fold axis in deep large cavity and in the sodalite unit, respectively, while additional one Te atom per unit cell was located at Te(3) opposite 4-ring in the large cavity.

Tellurium in the Sodalite Unit of $|Ca_6Te_3|[Si_{12}Al_{12}O_{48}]$-LTA: One Te atom per unit cell at Te(2) are found on the 3-fold axis in each sodalite unit of $|Ca_6Te_3|[Si_{12}Al_{12}O_{48}]$-LTA (see Figure 1(a)). The location of Te at Te(2), opposite 6-ring in the sodalite unit, is unambiguous, because no other chemically possible atoms or ions, such as Al and O, could account for the electron density (*ca*. 52) found at this position. The approach distance of this Te atom to 6-ring Ca^{2+} cation of the same 3-fold axis is 2.42(4) Å (see Table 3). Considering the radii of Ca^{2+} ($r_{Ca^{2+}}$ = 0.99 Å) and Te atom (1.43 Å),[35] the Te atom is sufficiently close to it's neighbors to be considered as having relatively strong interaction. This one Te atom at Te(2) on the inner surface of the sodalite unit in $|Ca_6Te_3|[Si_{12}Al_{12}O_{48}]$-LTA may be placed within their partially occupied equipoints in various ways. Provided that Te atoms are sorbed in 50% of all of sodalite units, then linear Te_2 clusters may exist. The shortest possible inter-Te distance, Te(2)-Te(2) = 1.98(5) Å, is impossibly short and is dismissed. Another inter-Te distance, 2.86(10) Å, suggests the possibility of an Te(2)-Te(2) interaction. A stereoview of Te_2 cluster in the sodalite unit of $|Ca_6Te_3|[Si_{12}Al_{12}O_{48}]$-LTA is shown in Figure 1(b). Furthermore, provided that Te atoms are sorbed in 25% of all of sodalite units, then tetrahedral Te_4 clusters may exist with a Te(2)-Te(2) distance of 2.86(10) Å, Ca(1)-Te(2)-Te(2) = 125.30(10)°, and Te(2)-Te(2)-Te(2) = 60° (see Table 3 and Figure 1(c)). All 4 Te atoms are associated with Ca^{2+} ions with a Ca(1)-Te(2) distance of 2.42(4) Å. Considering radii of these Te atoms, 1.43 Å,[35] those approach distances indicate that these Te atoms have somewhat large number of covalent contacts with other Te atoms and Ca^{2+} cations.

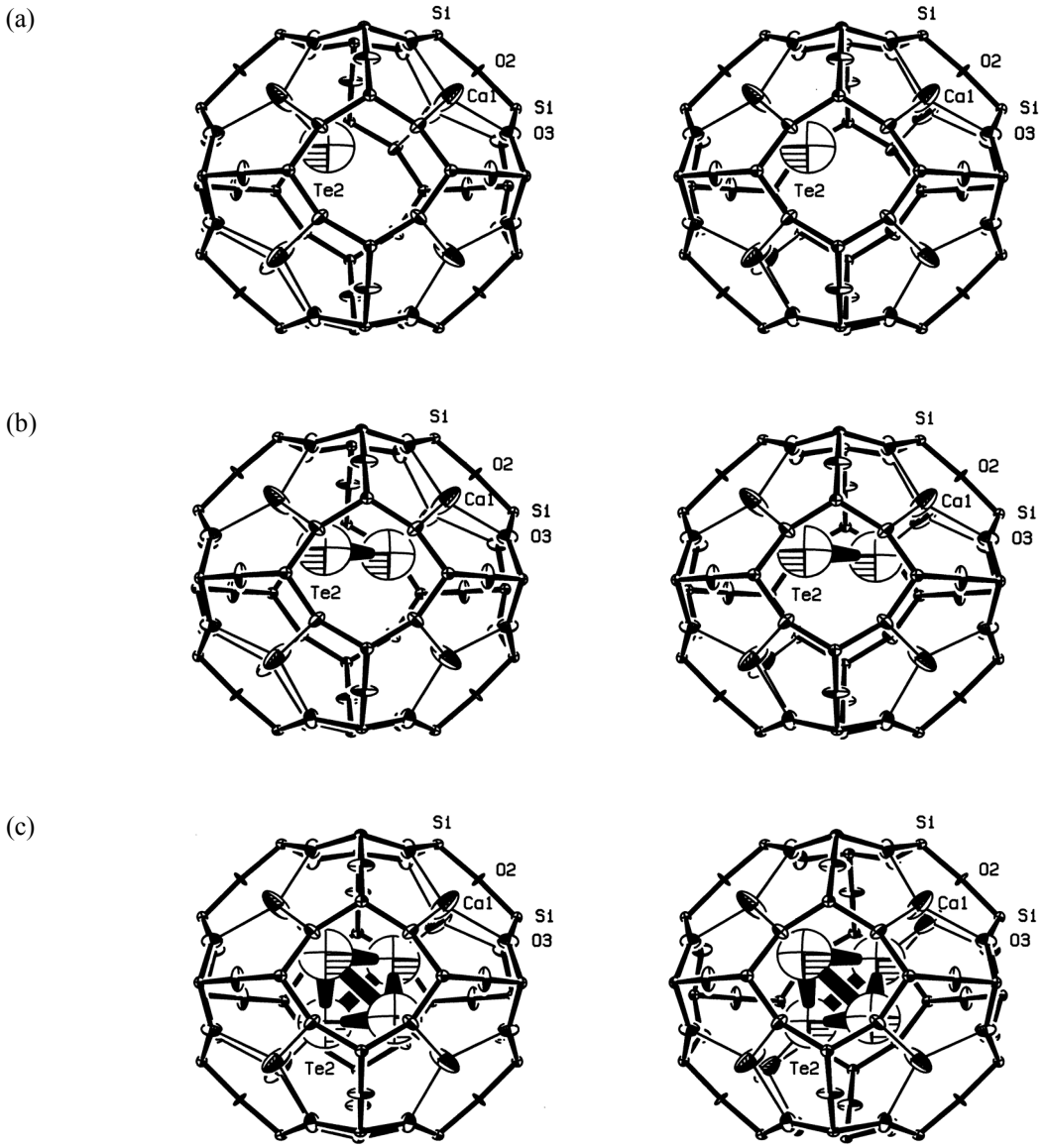

Figure 1. A stereoview of a sodalite unit in $|Ca_6Te_3|[Si_{12}Al_{12}O_{48}]$-LTA (100% (a), 50% (b), and 25% (c) of sodalite unit, crystal 1). The zeolite A framework is drawn with light bonds between oxygens and tetrahedrally coordinated (Si, Al) atoms. Ellipsoids of 20% probability are shown.

Telluriums in the Large Cavity of $|Ca_6Te_3|[Si_{12}Al_{12}O_{48}]$-LTA: The two atoms of Te in the large cavity of $|Ca_6Te_3|[Si_{12}Al_{12}O_{48}]$-LTA are found at two crystallographically distinct positions. That there are two kinds of positions indicates that the Te atoms are not arranging themselves by simple packing within the highly symmetric zeolites. It is attributed to dipolar interactions among the sorbed Te (*vide infra*). One Te atom at Te(1) lies on a 3-fold axis opposite a 6-ring and another Te atom at Te(3) lies opposite a 4-ring (see Figure 2(a) and (b)).

The closest approach of the Te atom to nonframework cation is 2.43(3) Å for Te(1)-Ca(1), while that to framework oxygen (Te(3)-O(1)) is 2.82(5) Å (see Table 3). Considering the radii of the cations ($r_{Ca^{2+}}$ = 0.99 Å), framework oxygens (1.32 Å), and Te atoms (1.43 Å),[35] the Te atoms are sufficiently close to their neighbors to be considered as having relatively strong interactions. In particular, when the distances are compared to the sum of the above radii for Ca^{2+} and Te, 0.99 + 1.43 = 2.42 Å,[35] the approach distance of the 3-fold axis Te atom, Te(1), to the 6-ring Ca^{2+} ion (2.43(3) Å) indicates relatively strong Ca^{2+}-Te interaction. This interaction between Te atom at Te(1) in the large cavity and 6-ring Ca^{2+} ion is very similar with the interaction between Te at Te(2) in the sodalite unit and 6-ring Ca^{2+} (Te(1)-Ca(1) = 2.43(3) and Te(2)-Ca(1) = 2.42(4) Å).

The two Te atoms at Te(1) and Te(3) on the inner surface of the large cavity may be placed within their partially occupied equipoints in various ways. The shortest inter-Te distance, Te(1)-Te(3) = 2.99(3) Å, is possible and suggests the possibility of an Te(1)-Te(3) interaction with favorably oriented induced dipoles (see Figure 2(a)). In this linear Te_2 cluster, Te atoms alternatively approach Ca^{2+} ion and 4-oxygen ring and are polarized oppositely, allowing their inter-Te approaches to be

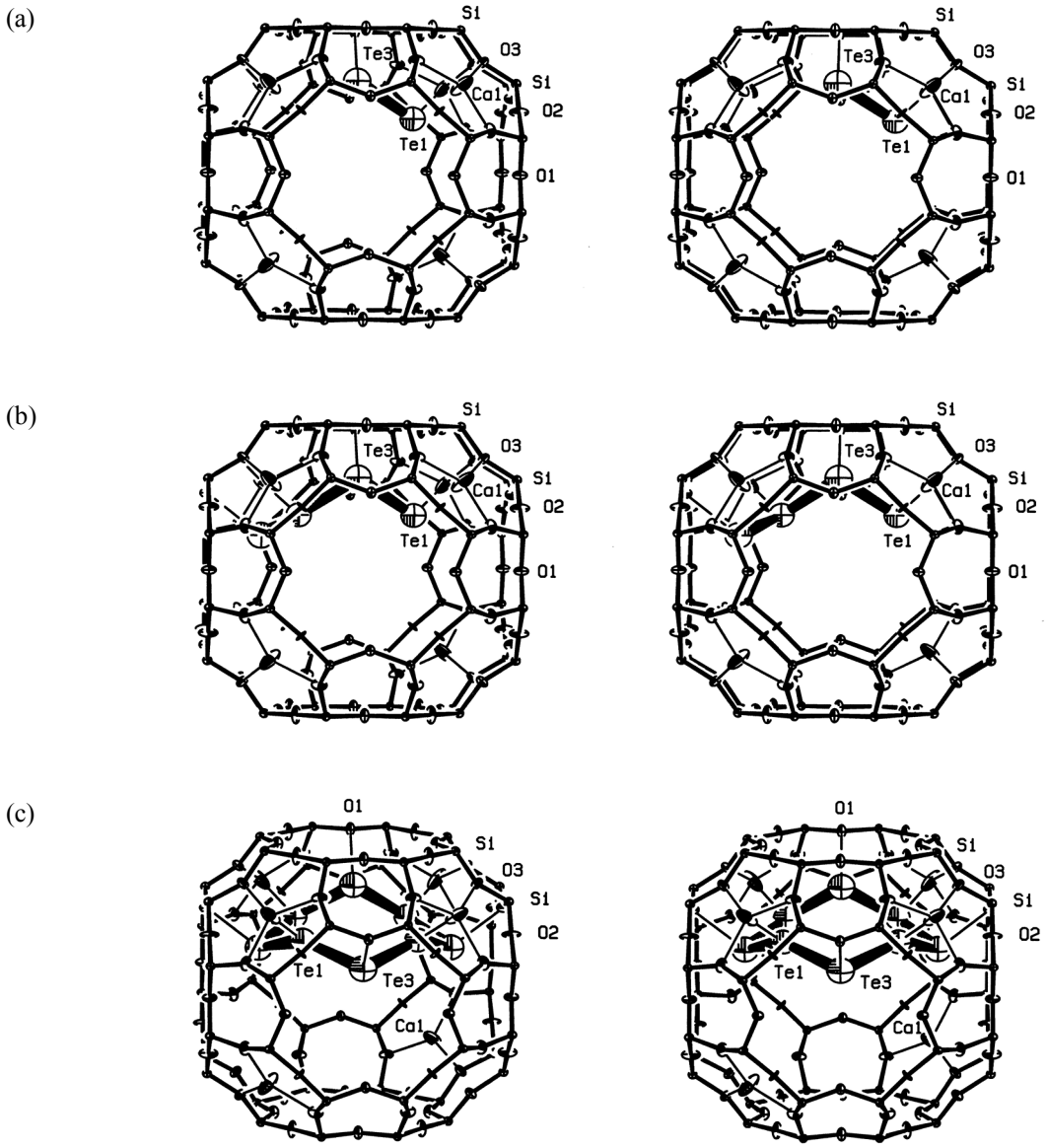

Figure 2. A stereoview of large cavity in $|Ca_6Te_3|[Si_{12}Al_{12}O_{48}]$-LTA (100% (a), 50% (b), and 25% (c) of large cavity, crystal 1). See the caption to Figure 1 for other details.

attractive, like $Ca(1)^{\delta+}$-$Te(1)^{\delta-}$-$Te(3)^{\delta+}$-$O(1)^{\delta-}$. The longer distances (4.76(1), 6.81(6), and 7.75(3) Å) are also possible.

Provided that Te atoms are sorbed in only 50% of all large cavities, then bent linear Te_4 clusters may exist. The 4 Te atoms at Te(1) and Te(3) on the inner surface of the large cavity may be placed in similar way to above. A distance found between Te(1) and Te(3), 2.99(3) Å, is also possible and suggests the possibility of an Te(1)-Te(3)-Te(1)-Te(3) interaction with favorably oriented induced dipoles (see Figure 2(b)). In this bent linear Te_4 cluster, Te atoms alternatively approach two Ca^{2+} ions and two 4-oxygen rings; they are therefore polarized oppositely, allowing their inter-Te approaches to be attractive, like $Ca(1)^{\delta+}$-$Te(1)^{\delta-}$-$Te(3)^{\delta+}$-$Te(1)^{\delta-}$-$Te(3)^{\delta+}$-$O(1)^{\delta-}$.

If 25% of the large cavity is sorbed by Te atoms, the most favorable arrangement of 8 Te atoms is a butterflyshape, [-Te(1)-Te(3)-Te(1)-Te(3)-Te(1)-Te(3)-Te(1)-Te(3)-], Te(1)-Te(3) = 2.99(3) Å, and Te(1)-Te(3)-Te(1) = 103.4(16)°, because of its higher symmetry and the considerations regarding alternating polarizations of Te atoms as seen in Figure 2(c).

Crystal Structure of $|Ca_{46}Te_8|[Si_{100}Al_{92}O_{384}]$-FAU (Crystal 2). Zeolite X is a synthetic Al-rich analogue of the naturally occurring mineral faujasite. The 14-hedron with 24 vertices known as the sodalite cavity or β cage may be viewed as the principal building block of the aluminosilicate framework of the zeolite (see Figure 3). These sodalite units are connected tetrahedrally at 6-rings by bridging oxygens to give double 6-rings (D6Rs, hexagonal prisms) and, concomitantly, an interconnected set of even larger cavities (supercages) accessible in three dimensions through 12-ring (24-membered) windows. The Si and Al atoms occupy the vertices of these polyhedra. The oxygen atoms lie approximately halfway between each pair of Si and Al atoms but are displaced from those points to give near tetrahedral angles about Si and Al.

Exchangeable cations that balance the negative charge of

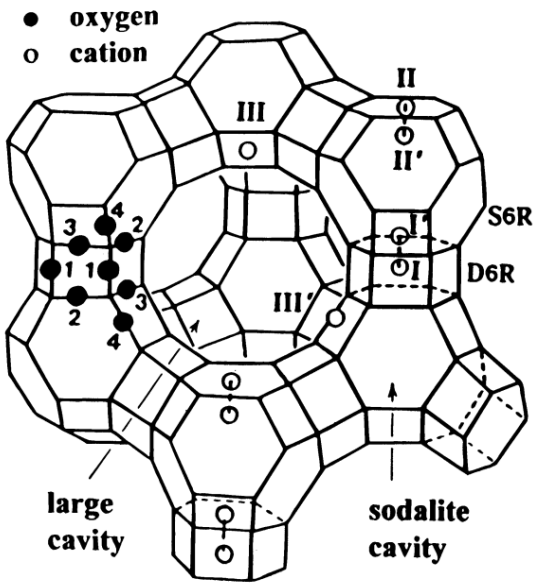

Figure 3. Stylized drawing of the framework structure of zeolite X. Near the center of the each line segment is an oxygen atom. The different oxygen atoms are indicated by the numbers 1 to 4. Silicon and aluminum atoms alternate at the tetrahedral intersections, with the exception that Si substitutes for Al at about 4% of the Al positions. Extraframework cation positions are labeled with Roman numbers.

the aluminosilicate framework are found within the zeolite's cavities. They are usually found at the following sites shown in Figure 3: site I at the center of the D6R, I' in the sodalite cavity on the opposite side of either of the D6R's six-rings from site I, II' inside the sodalite cavity near a single 6-ring (S6R) entrance to the supercage, II opposite a S6R in the supercage, III on a 2-fold axis opposite an -O(3)-O(4)-O(3)-O(4)- 4-ring (between two 12-rings) in the supercage, and III' somewhat or substantially off the 2-fold axis but otherwise on the inner surface of the supercage or near a 12-ring.

The mean values of the Si-O bond lengths are normal, 1.618(15) Å and 1.704(14) Å, respectively. The individual bond lengths, however, show meaningful variations: Si-O from 1.581(15) to 1.647(15) Å and Al-O from 1.685(13) to 1.720(14) Å (see Table 3). This effect is commonly observed. In the crystal structures of the ethylene and acetylene sorption complexes of dehydrated $|Ca_{46}|[Si_{100}Al_{92}O_{384}]$-FAU,[36] the mean values of the Si-O and Al-O bond lengths are 1.65 and 1.70 Å, respectively, and similar variations are seen. The Si-O and Al-O distances depend upon Ca^{2+} coordination to framework oxygen: Ca^{2+} ions coordinate only to O(2) and O(3) causing their bonds to Si and Al to lengthen. Only small changes in the framework geometry are observed upon tellurium sorption.

The 46 Ca^{2+} ions per unit cell are found at four crystallographic sites. The 3 Ca^{2+} ions at Ca(1) lie on the 16-fold sites I at the centers of the D6Rs. The octahedral Ca(1)-O(3) distance, 2.677(16) Å, is just a little longer than the sum of the corresponding ionic radii, 0.99 + 1.32 = 2.31 Å,[35] indicating a reasonably good fit (see Figure 4). The 21 Ca^{2+} ions at Ca(2) fill the 32 equivalent positions of site I' in the sodalite unit; these Ca^{2+} ions are 2.500(17) Å from their nearest neighbors, three O(3) framework oxygens. The remaining 10 and 12 Ca^{2+} ions at Ca(3) and Ca(4), respectively, fill the 32 equivalent positions of site II. The distances of Ca^{2+} at Ca(3) and Ca(4) to the nearest framework oxygens are 2.233(15) and 2.62(3) Å for Ca(3)-O(2) and Ca(4)-O(2), respectively. Each of the Ca^{2+} ions at Ca(2) extends 1.34 Å into the sodalite unit from the plane of its three O(3) framework oxygens (see Table 4). Each of the Ca^{2+} ions at Ca(3) and Ca(4) extends 0.20 and 1.33 Å, respectively, into the supercage from the plane of its three O(2) framework oxygens (see Table 4).

The Te atoms are found at three crystallographically distinct positions: 4 Te atoms at Te(1) per unit cell are located opposite double 6-rings in the sodalite unit and four at Te(2) and Te(3) per unit cell are located general positions in the supercage.

Tellurium in the Sodalite Unit of $|Ca_{46}Te_8|[Si_{100}Al_{92}O_{384}]$-FAU: Four Te atoms per unit cell at Te(1) are found on the 3-fold axes in the sodalite units. Only 50% of sodalite units of $|Ca_{46}Te_8|[Si_{100}Al_{92}O_{384}]$-FAU has one Te atom because each unit cell of zeolite X has 8 sodalite units (see Figure 5(a)). The location of Te at Te(1), opposite 6-ring in the sodalite unit, is

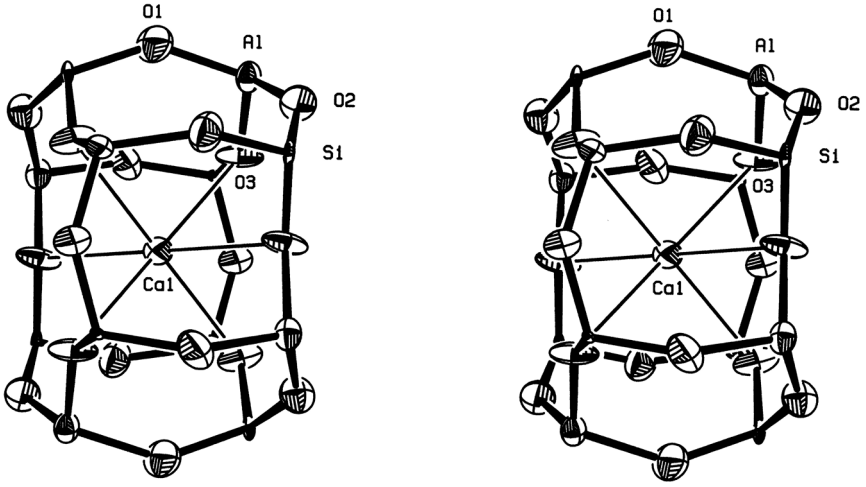

Figure 4. A stereoview of hexagonal prism in $|Ca_{46}Te_8|[Si_{100}Al_{92}O_{384}]$-FAU (crystal 2). See the caption to Figure 1 for other details.

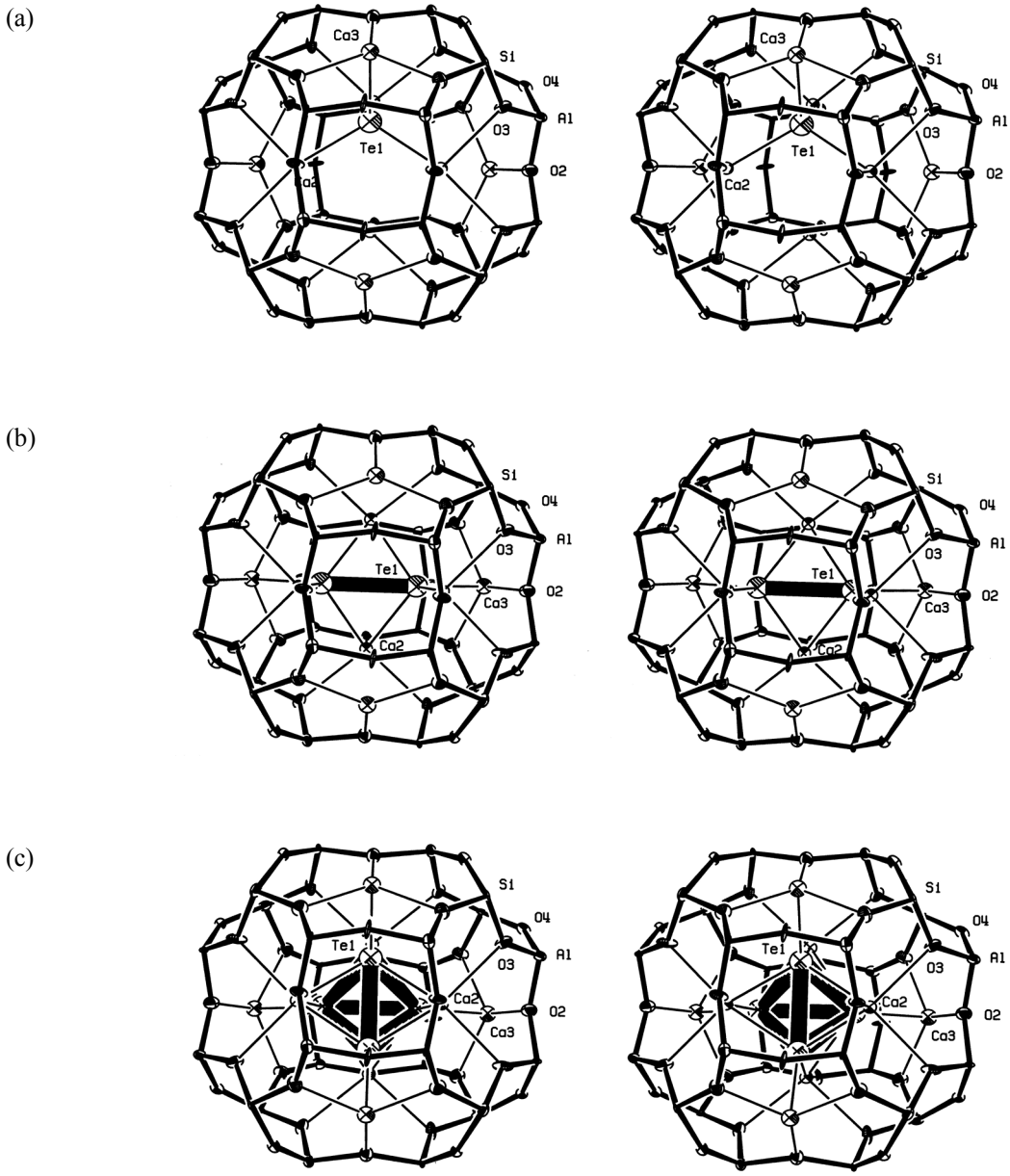

Figure 5. A stereoview of sodalite unit in $|Ca_{46}Te_8|[Si_{100}Al_{92}O_{384}]$-FAU (50% (a), 25% (b), and 12.5% (c) of sodalite unit, crystal 2). See the caption to Figure 1 for other details.

unambiguous, because no other chemically possible atoms or ions, such as Al and O, could account for the electron density (*ca*. 52) found at this position. The approach distances of this Te atom to 6-ring Ca^{2+} ion of the same 3-fold axis at Ca(3) and another 3-fold axis at Ca(2) are 2.479(4) and 2.458(14) Å, respectively (see Table 3). Considering the radii of Ca^{2+} ($r_{Ca}{}^{2+}$ = 0.99 Å) and Te atom (1.43 Å),[35] the Te atom is sufficiently close to it's neighbors to be considered as having relatively strong interaction. This one Te atom at Te(1) on the inner surface of the sodalite unit in $|Ca_{46}Te_8|[Si_{100}Al_{92}O_{384}]$-FAU may be placed within their partially occupied equipoints in various ways. Provided that Te atoms are sorbed in 25% of all of sodalite units, then linear Te_2 cluster may exist (see Figure 5(b)). The possible inter-Te distance, 2.69(4) Å, suggests the possibility of an Te(2)-Te(2) interaction. A stereoview of Te_2 cluster in the sodalite unit of $|Ca_{46}Te_8|[Si_{100}Al_{92}O_{384}]$-FAU is shown in Figure 5(b). Furthermore, provided that Te atoms are sorbed in 12.5% of all of sodalite units, then tetrahedral Te_4 clusters may exist with Te(1)-Te(1) = 2.69(4) Å, Ca(2)Te(1)-Te(1) = 105.5(6)°, and Te(1)-Te(1)-Te(1) = 60° (see Table 3 and Figure 5(c)). Each Te atom is associated with 2 Ca^{2+} ions at Ca(2) and 2 at Ca(3) tetrahedrally with 2.458(14) and 2.479(4) Å for Ca(2)-Te(1) and Ca(3)-Te(1), respectively. On considering the radii of these Te atoms, 1.43 Å,[35] those approach distances indicate that these Te atoms have somewhat large number of covalent contacts with other Te atoms and Ca^{2+} cations.

Telluriums in the Supercage of $|Ca_{46}Te_8|[Si_{100}Al_{92}O_{384}]$-FAU: The 4 atoms of Te in the supercage of $|Ca_{46}Te_8|[Si_{100}Al_{92}O_{384}]$-FAU are found at two crystallographically distinct

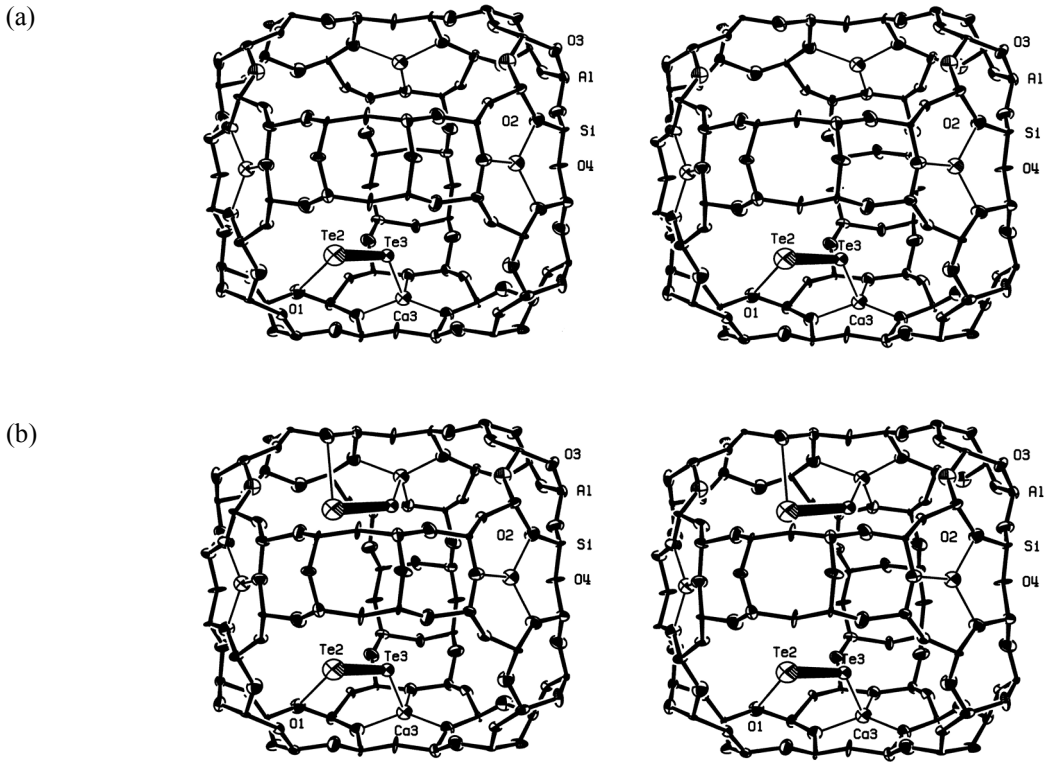

Figure 6. A stereoview of supercage in $|Ca_{46}Te_8|[Si_{100}Al_{92}O_{384}]$-FAU (25% (a) and 12.5% (b) of supercage, crystal 2). See the caption to Figure 1 for other details.

positions. That there are two kinds of positions indicates that the Te atoms are not arranging themselves by simple packing within the highly symmetric zeolites. It is attributed to dipolar interactions among the sorbed Te (*vide infra*). Two Te atoms at Te(2) and the remaining 2 Te atoms at Te(3) lie on general positions in the supercage (see Figure 6(a) and (b)). Provided that Te atoms are sorbed in 25 or 12.5% of supercages, then Te_2 or two Te_2 clusters, respectively, may exist.

The closest approach of the Te atom to nonframework cation is 2.26(7) Å for Te(3)-Ca(3), while that to framework oxygen (Te(2)-O(1)) is 3.27(7) Å (see Table 3). Considering the radii of the cations ($r_{Ca^{2+}}$ = 0.99 Å), framework oxygens (1.32 Å), and tellurium atoms (1.43 Å),[35] the Te atoms are sufficiently close to their neighbors to be considered as having relatively strong interactions. In particular, when the distances are compared to the sum of the above radii for Ca^{2+} and Te, 0.99 + 1.43 = 2.42 Å,[35] the approach distance of the Te atom at Te(3), to the 6-ring Ca^{2+} ion at Ca(3) (2.26(7) Å) indicates very strong Ca^{2+}-Te interaction. This interaction between Te atom at Te(3) in the supercage and 6-ring Ca^{2+} ion at Ca(3) is much more stronger than the interaction between Te at Te(1) in the sodalite unit and 6-ring Ca^{2+} (Te(1)-Ca(2) = 2.458(14) Å and Te(1)-Ca(3) = 2.479(4) Å).

The 2 Te atoms at Te(2) and Te(3) on the inner surface of the supercage may be placed within their partially occupied equipoints in various ways. The shortest possible inter-Te distance, Te(2)-Te(3) = 2.31(3) Å, is impossibly short and dismissed. Another inter-Te distance, 2.760(11) Å, suggests the possibility of an Te(2)-Te(2) interaction. In this linear Te_2 cluster, Te atoms alternatively approach Ca^{2+} ion at Ca(3) and 4-oxygen ring and are polarized oppositely, allowing their inter-Te approaches to be attractive like as this $Ca(3)^{\delta+}$-$Te(3)^{\delta-}$-$Te(2)^{\delta+}$-$O(1)^{\delta-}$ (see Figure 6(a)). The longer distances (4.78(14), 5.0(3), 7.9(5), 8.0(7), and 8.2(3) Å) is also possible.

Provided that Te atoms are sorbed in only 12.5% of all supercages, then two Te_2 clusters may exist (see Figure 6(b)).

Summary

Single crystals of fully dehydrated and fully Ca^{2+}-exchanged zeolites A ($|Ca_6|[Si_{12}Al_{12}O_{48}]$-LTA) and X ($|Ca_{46}|[Si_{100}Al_{92}O_{384}]$-FAU) were reacted with Te at 623 K and 673 K for 5 days, respectively. Crystal structures of Te-sorbed Ca^{2+}-exchanged zeolites A and X have been determined by single-crystal X-ray diffraction techniques in the cubic space group $Pm\bar{3}m$ and $Fd\bar{3}$, respectively. The crystal structures of $|Ca_6Te_3|[Si_{12}Al_{12}O_{48}]$-LTA and $|Ca_{46}Te_8|[Si_{100}Al_{92}O_{384}]$-FAU have been refined to the final error indices of R_1/wR_2 = 0.1096/ 0.2768 and R_1/wR_2 = 0.1054/0.2979 with 204 and 282 reflections for which $F_o > 4\sigma(F_o)$, respectively. In the crystal structure of Te-sorbed Ca^{2+}-exchanged zolite A ($|Ca_6Te_3|[Si_{12}Al_{12}O_{48}]$-LTA), a total of three sorbed Te atoms per unit cell found at two different 3-fold positions and at 24-fold positions. One Te atom per unit cell was found at Te(1) on the 3-fold axis in deep large cavity and the other Te atom at Te(2) was found on the 3-fold axis in the sodalite unit. Additional one Te atom per unit cell was located at Te(3) opposite 4-ring in the large cavity. In the crystal structure of Te-sorbed Ca^{2+}-exchanged zeolite X ($|Ca_{46}Te_8|[Si_{100}Al_{92}O_{384}]$-FAU), 8 Te atoms are found at three crystallographically distinct positions: 4 at Te(1) per unit cell

are located opposite double 6-rings in the sodalite unit and 4 Te atoms at Te(2) and Te(3) per unit cell are located general positions in the supercage.

The Te clusters in zeolites A and X are stabilized by interaction with cations and framework oxygen. In sodalite units, Te-Te distances of 2.86(10) and 2.69(4) Å in zeolites A and X, respectively, exhibited strong covalent property due to their interaction with Ca^{2+} ions. On the other hand, in large cavity and supercage, those of 2.99(3) and 2.76(11) Å in zeolites A and X, respectively, showed ionic property because alternative ionic interaction was formed through framework oxygen at one end and Ca^{2+} ions at the other end.

Acknowledgments. We gratefully acknowledge the support of the Central Laboratory of Kyungpook National University for the diffractometer and computing facilities. This study was carried out with the support of Cooperative Research Program for Agricultural Science & Technology Development (200901OFT102966074), RDA, Republic of Korea.

Supplementary Material Available. Tables of calculated and observed structure factors (18 pages). The supporting materials will be given upon your request to a corresponding author (Tel: +82-54-820-5454, Fax: +82-54-822-5452, e-mail: wtlim @andong.ac.kr).

References

1. Almand, P.; Saboungi, M. L. *Physical Review Letters* **1997**, *79*, 2061-2064 and references therein.
2. Wang, Y.; Herron, N. *J. Phys. Chem*. **1987**, *91*, 257-260.
3. Parise, J. B.; MacDougall, J. E.; Herron, N.; Farlee, R.; Sleight, A. W.; Wang, Y.; Bein, T.; Moller, K.; Moroney, L. M. *Inorg. Chem*. **1988**, *27*, 221-228.
4. Herron, N. *Journal of Inclusion Phenomena and Molecular Recognition in Chemistry* **1995**, *21*, 283-298.
5. Chen, W.; Wang, Z.; Lin, Z.; Lin, L.; Fang, K.; Xu, Y.; Su, M.; Lin, J. *J. Appl. Phys*. **1998**, *83*, 3811-3815 and reference therein.
6. Tani, T.; Murofushi, M. *J. Imaging Sci. Technol*. **1994**, *38*, 1-9.
7. Takahashi, K.; Miyahara, J.; Shibahara, Y. *J. Electrochem. Soc*. **1985**, *132*(6), 1492-1494.
8. Zadorozhnii, A. I.; Panina, L. K.; Sakash, V. F.; Strakhov, L. P.; Kholodkevich, S. V. *Sov. Phys. Solid State* **1980**, *22*(10), 1713-1715.
9. Goldbach, A.; Iton, L.; Grimsditch, M.; Saboungi, M. L. *J. Am. Chem. Soc*. **1996**, *118*, 2004-2007.
10. Bogomolov, V. N.; Kholodkevich, S. V.; Romanov, S. G.; Agroskin, L. S. *Solid State Communications* **1983**, *47*(3), 181-182.
11. Tamura, K.; Hosokawa, S.; Endo, H.; Yamasaki, S.; Oyanagi, H. *Journal of the Physical Society of Japan* **1986**, *55*(2), 528-533.
12. Wang, Y.; Herron, N. *J. Phys. Chem*. **1987**, *91*, 5005-5008.
13. Bogomolov, V. N.; Lutsenko, E. L.; Petranovskii, V. P.; Kholodkevich, S. V. *JETP Lett*. **1976**, *23*(9), 482-484.
14. Bogomolov, V. N.; Zadorozhnii, A. I.; Petranovskii, V. P.; Fokin, A. V.; Kholodkevich, S. V. *JETP Lett*. **1979**, *29*(7), 373-375.
15. Bogomolov, V. N.; Poborchy, V. V.; Romanov, S. G.; Shagin, S. I. *J. Phys. C: Solid State Phys*. **1985**, *18*, L313-L317.
16. Terasaki, O.; Yamazaki, K.; Thomas, J. M.; Ohsuna, T.; Watanabe, D.; Sanders, J. V.; Barry, J. C. *Nature* **1987**, *330*, 58-60.
17. Terasaki, O.; Yamazaki, K.; Thomas, J. M.; Ohsuna, T.; Watanabe, D.; Sanders, J. V.; Barry, J. C. *Journal of Solid State Chemistry* **1988**, *77*, 72-83.
18. Bogomolov, V. N.; Efimov, A. N.; Ivanova, M. S.; Poborchii, V. V.; Romanov, S. G.; Smolin, Yu. I.; Shepelev, Yu. F. *Sov. Phys. Solid State* **1992**, *34*(6), 916-919.
19. Lee, S. H. M. E. Thesis, Kyungpook National University, 1999.
20. Poborchii, V. V. *Solid State Communications* **1998**, *107*(9), 513-518.
21. Nouze, Y.; Kodaira, T.; Terasaki, O.; Yamazaki, K.; Goto, T.; Watanabe, D.; Thomas, J. M. *J. Phys.: Condens. Matter* **1990**, *2*(23), 5209-5217.
22. Lin, Z.; Wang, Z.; Chen, W.; Lir, L.; Li, G.; Liu, Z.; Han, H.; Wang, Z. *Solid State Communications* **1996**, *100*(12), 841-843.
23. Charnell, J. F. *J. Crystal. Growth* **1971**, *8*, 291-294.
24. Bogomolov, V. N.; Petranovskii, V. P. *Zeolites* **1986**, *6*, 418-419.
25. Cruz, W. V.; Leung, P. C. W.; Seff, K. *J. Am. Chem. Soc*. 1978, *100*, 6997-7003.
26. Mellum, M. D.; Seff, K. *J. Phys. Chem*. 1984, *88*, 3560-3563.
27. Kwon, J. H.; Jang, S. B.; Kim, Y.; Seff, K. *J. Phys. Chem*. 1996, *100*, 13720-13724.
28. Sheldrick, G. M. *SHELXL97*, *Program for the Refinement of Crystal Structures*; University of Gottingen: Germany, 1997.
29. Firor, R. L.; Seff, K. *J. Am. Chem. Soc*. **1978**, *100*, 3091-3096.
30. Doyle, P. A.; Turner, P. S. *Acta Crystallogr*., *Sect. A* **1968**, *24*, 390-397.
31. *International Tables for X-ray Crystallography*; Ibers, J. A.; Hamilton, W. C., Eds.; Kynoch Press: Birmingham, England, 1974; Vol. IV, pp 71-98.
32. Cromer, D. T. *Acta Crystallogr.* **1965**, *18*, 17-23.
33. *International Tables for X-ray Crystallography*; Kynoch Press: Birmingham, England, 1974; Vol. IV, pp 148-150.
34. Lee, S. H.; Kim, Y.; Kim, D. S.; Seff, K. *Bull. Korean Chem. Soc*. 1998, *19*(1), 98-103.
35. *Handbook of Chemistry and Physics*, 70th ed.; The chemical Rubber Co.: Cleveland, OH, 1989/1990; p F-18.
36. Jang, S. B.; Jeong, M. S.; Kim, Y.; Seff, K. *J. Phys. Chem. B* **1997**, *101*, 3091-3096.